The Astrophysical Journal, 730:8 (13pp), 2011 March 20 doi:10.1088/0004-637X/730/1/8

ON THE REDSHIFT EVOLUTION OF THE Lyα ESCAPE FRACTION AND THE DUST CONTENT OF GALAXIES

Matthew Hayes[1], Daniel Schaerer[1,2], Göran Östlin[3], J. Miguel Mas-Hesse[4], Hakim Atek[5], and Daniel Kunth[6]
[1] Observatory of Geneva, University of Geneva, 51 chemin des Maillettes, 1290 Versoix, Switzerland; matthew.hayes@unige.ch
[2] Laboratoire d'Astrophysique de Toulouse-Tarbes, Université de Toulouse, CNRS, 14 Avenue E. Belin, 31400 Toulouse, France
[3] Oskar Klein Centre, Department of Astronomy, AlbaNova University Center, Stockholm University, 10691 Stockholm, Sweden
[4] Centro de Astrobiología (CSIC-INTA), P. O. Box 78, 28691 Villanueva de la Cañada, Madrid, Spain
[5] Spitzer Science Center, Caltech, Pasadena, CA 91125, USA
[6] Institut d'Astrophysique de Paris (IAP), 98 bis boulevard Arago, 75014 Paris, France
Received 2010 August 17; accepted 2010 December 23; published 2011 February 24

ABSTRACT

The Lyα emission line has been proven to be a powerful tool for studying evolving galaxies at the highest redshift. However, in order to use Lyα as a physical probe of galaxies, it becomes vital to know the Lyα escape fraction ($f_{\rm esc}^{\rm Ly\alpha}$). Unfortunately, due to the resonant nature of Lyα, $f_{\rm esc}^{\rm Ly\alpha}$ may vary unpredictably and requires empirical measurement. Here, we compile Lyα luminosity functions (LFs) between redshifts $z = 0$ and 8 and, combined with Hα and ultraviolet data, assess how $f_{\rm esc}^{\rm Ly\alpha}$ evolves with redshift. We find a strong upward evolution in $f_{\rm esc}^{\rm Ly\alpha}$ over the range $z = 0.3$–6, which is well fit by the power law $f_{\rm esc}^{\rm Ly\alpha} \propto (1+z)^{\xi}$ with $\xi = (2.57^{+0.19}_{-0.12})$. This predicts that $f_{\rm esc}^{\rm Ly\alpha}$ should reach unity at $z = 11.1$. By comparing $f_{\rm esc}^{\rm Ly\alpha}$ and E_{B-V} in individual galaxies we derive an empirical relationship between $f_{\rm esc}^{\rm Ly\alpha}$ and E_{B-V}, which includes resonance scattering and can explain the redshift evolution of $f_{\rm esc}^{\rm Ly\alpha}$ between $z = 0$ and 6 purely as a function of the evolution in the dust content of galaxies. Beyond $z \approx 6.5$, $f_{\rm esc}^{\rm Ly\alpha}$ drops more substantially, an effect attributed to either ionizing photon leakage, or an increase in the neutral gas fraction of the intergalactic medium. While distinguishing between these two scenarios may be extremely challenging, by framing the problem this way we remove the uncertainty of the halo mass from Lyα-based tests of reionization. We finally derive a new method by which to estimate the dust content of galaxies, based purely upon the observed Lyα and UV LFs. These data are characterized by an exponential with an *e*-folding scale of $z_{\rm EBV} \approx 3.4$.

Key words: dark ages, reionization, first stars – galaxies: evolution – galaxies: high-redshift – galaxies: luminosity function, mass function – galaxies: star formation

Online-only material: color figures

1. INTRODUCTION

Surveys targeting the Lyα emission line show unique profitability for examining the formation and evolution of the galaxy population between redshifts $z \approx 2$ and $\gtrsim 7$. Lyα has been exploited by many teams and the combined catalogs would currently include over 2000 entries (e.g., Venemans et al. 2002; Hu et al. 2004; van Breukelen et al. 2005; Wang et al. 2005; Shimasaku et al. 2006; Gronwall et al. 2007; Ouchi et al. 2008; Nilsson et al. 2009; Guaita et al. 2010; Cassata et al. 2011; Hayes et al. 2010a). Wherever such large samples are available, the temptation is strong to use their statistical power to examine as many physical properties of the galaxy population as possible. This, however, requires that the numbers one has at hand are in some way a physical reflection of those underlying properties; to first order the luminosity (and/or equivalent width for emission lines) must be related to its intrinsic value. For surveys that target the rest-frame ultraviolet (UV) continuum, this is simply a matter of applying a dust correction. However, the resonant nature of the Lyα line means that its radiation transport becomes an involved and detailed problem (Osterbrock 1962; Adams 1972; Harrington 1973; Neufeld 1990; Ahn et al. 2003; Verhamme et al. 2006; Tasitsiomi 2006; Laursen et al. 2009). This further implies that the escaping fraction of photons ($f_{\rm esc}^{\rm Ly\alpha}$) may not be treated as a straightforward function of the dust content, is liable to evolve strongly with an evolving galaxy population, and must be measured empirically. Pursuing this line of inquiry, the evolution of $f_{\rm esc}^{\rm Ly\alpha}$ can therefore provide us with independent estimates of how various properties of the galaxy population evolve over cosmic time.

Since Lyα photons scatter in neutral hydrogen (H I) until they either escape or are absorbed by dust grains, most fundamentally the radiation transport depends upon the H I content, its geometry and kinematics, and the dust content and distribution. Regrettably, with current observational facilities, the only one of these quantities that can easily be estimated for large samples of high-redshift galaxies is the dust attenuation, which is typically derived from the stellar continuum. Consequently, the amalgamated effects of the remaining quantities, and how they affect $f_{\rm esc}^{\rm Ly\alpha}$, can only be assessed on a statistical basis.

Lyα surveys have been fruitful over the last decade, but it is only very recently that robust $f_{\rm esc}^{\rm Ly\alpha}$ measurements have been made on statistically meaningful samples (Verhamme et al. 2008; Atek et al. 2009; Kornei et al. 2010; Hayes et al. 2010a). However, at the current juncture, all of these studies estimate $f_{\rm esc}^{\rm Ly\alpha}$ by different methods, and are derived among samples compiled at various redshifts and filtered through differing selection functions. Thus, synthesis of the results remains somewhat difficult. Furthermore, there is no self-consistent study in the current literature of how $f_{\rm esc}^{\rm Ly\alpha}$ evolves with redshift, and with the present paper we take the first steps toward rectifying this. We begin by compiling various Lyα, Hα, and UV data sets in Section 2, which we use to estimate

the redshift evolution of $f_{\rm esc}^{\rm Ly\alpha}$. We discuss the general trends and draw comparisons with other observational and theoretical methods in Section 3. In Section 4, we investigate the effect of the one quantity that is relatively easy to measure—the dust content—and discuss how it affects $f_{\rm esc}^{\rm Ly\alpha}$. In Section 5, we discuss the trends with redshift in more detail and synthesize information from Sections 3 and 4 in order to make more detailed inferences about the evolution of the properties of the interstellar medium (ISM) of galaxies, the intergalactic medium (IGM), and the overall dust content. In Section 6, we present a final summary. All data are scaled to a cosmology of $(H_0, \Omega_{\rm M}, \Omega_\Lambda) = (70\,{\rm km\,s^{-1}\,Mpc^{-1}}, 0.3, 0.7)$.

2. METHOD: THE LYα ESCAPE FRACTION MEASUREMENTS

2.1. Escape Fraction Calculations

We now proceed to compile various estimates of $f_{\rm esc}^{\rm Ly\alpha}$ as a function of redshift, but first we present the formalism. We continue with the Hayes et al. (2010a) definition of $f_{\rm esc}^{\rm Ly\alpha}$: the sample-averaged, "volumetric" escape fraction. This quantity is defined as the ratio of observed to intrinsic Lyα luminosity densities ($\rho_{\rm L}$), derived by integration over luminosity functions (LFs), as in Equation (1):

$$f_{\rm esc}^{\rm Ly\alpha} = \frac{\rho_{\rm L,Ly\alpha}^{\rm Obs}}{\rho_{\rm L,Ly\alpha}^{\rm Int}} = \frac{\int_{L_{\rm lo}}^{\infty} \Phi(L)_{\rm Ly\alpha}^{\rm Obs} \times L \times dL}{\int_{L_{\rm lo}}^{\infty} \Phi(L)_{\rm Ly\alpha}^{\rm Int} \times L \times dL}, \quad (1)$$

where $\Phi(L)$ are the standard LFs.[7] Thus, $f_{\rm esc}^{\rm Ly\alpha}$ is not simply a re-scaling of the LF by L (constantly scaling the escape fraction of all galaxies) or by Φ (the duty cycle scenario; see Nagamine et al. 2010 for examples of both of these methods). Instead, since $f_{\rm esc}^{\rm Ly\alpha}$ is simply defined as the ratio of luminosity densities, it can be thought of as the fraction of Lyα photons that escape from the survey volume, regardless of whether all galaxies show low $f_{\rm esc}^{\rm Ly\alpha}$, or whether only a fraction of galaxies are in the Lyα-emitting phase with high individual $f_{\rm esc}^{\rm Ly\alpha}$ (see arguments in Tilvi et al. 2009). By this definition, $f_{\rm esc}^{\rm Ly\alpha}$ also includes any possible effect that the IGM may have on the measured Lyα emission from galaxies. However, it is clear that the bulk of the evolution of $f_{\rm esc}^{\rm Ly\alpha}$ with redshift found in this paper can clearly not be attributed to variations of the IGM transmission.

Where possible (i.e., $z < 2.3$) we make a direct comparison between Lyα and Hα. We apply the most appropriate dust correction to Hα and multiply by the case B recombination ratio of Lyα/Hα = 8.7 (Brocklehurst 1971) in order to obtain the intrinsic Lyα. That is,

$$f_{\rm esc}^{\rm Ly\alpha}(z < 2.3) = \frac{\rho_{\rm L,Ly\alpha}^{\rm Obs}}{8.7 \times \rho_{\rm L,H\alpha}^{\rm Int}} = \frac{\rho_{\rm L,Ly\alpha}^{\rm Obs}}{8.7 \times 10^{0.4 E_{B-V} k_{6563}} \cdot \rho_{\rm L,H\alpha}^{\rm Obs}}, \quad (2)$$

where E_{B-V} must be the dust attenuation computed for the Hα-emitting sample, and k_{6563} is the extinction coefficient at the wavelength of Hα. Superscripts "Int" and "Obs" refer to the intrinsic and observed quantities.

At $z \gtrsim 2.3$, we are unable to obtain Hα LFs in order to use line ratios to estimate $f_{\rm esc}^{\rm Ly\alpha}$, and instead the estimate is derived from the UV continuum. This is a less elegant method since the conversion between UV and Lyα requires the assumption of a metallicity, initial mass function (IMF), and evolutionary stage. However, in light of the fact that higher redshift Hα studies will remain impossible until the arrival of the *James Webb Space Telescope*, this is the only way to proceed. It is fortunate that there is no evidence that IMFs should differ between Lyα- and UV-selected populations, although metallicities have been shown to be around 0.2 dex lower (e.g., Cowie et al. 2010), which translates into a difference of $\lesssim$20% in the intrinsic Lyα/UV ratio (Leitherer et al. 1999). For "normal" metallicities and IMFs, and assuming that on average star formation is ongoing at equilibrium, this method is the same as taking the ratio of Lyα/UV star formation rate densities (SFRDs), $\dot{\rho}_\star$:

$$f_{\rm esc}^{\rm Ly\alpha}(z > 2.3) = \frac{\dot{\rho}_{\star,\rm Ly\alpha}^{\rm Obs}}{\dot{\rho}_\star^{\rm Int}} = \frac{\dot{\rho}_{\star,\rm Ly\alpha}^{\rm Obs}}{10^{0.4 E_{B-V} k_{\rm UV}} \times \dot{\rho}_{\star,\rm UV}^{\rm Obs}}, \quad (3)$$

where now E_{B-V} must be the extinction seen by the UV-selected population and $k_{\rm UV}$ is the extinction coefficient in the UV.

The UV is of course not the only wavelength we can use for this experiment, but we choose to work exclusively with UV LFs since they (1) are so abundant in the literature, (2) have reasonably well understood selection functions, and (3) span an appropriately large range in redshift. We adopt UV measurements at redshifts most appropriate to our compiled Lyα data and dust attenuations derived from these samples themselves. We further adopt the dust attenuation law of Calzetti et al. (2000), and the star formation rate (SFR) calibrations of Kennicutt (1998). These calibrations assume a stabilized star formation episode at a constant rate for longer than around 100 Myr, with a Salpeter IMF (mass limits between 0.1 and 100 $M_\odot$), and a complete ionization efficiency (no leaking and no destruction of ionizing photons by dust). In general, we assume that "UV" refers to the rest-frame wavelength of 1500 Å, where the extinction coefficient computed from the relationship of Calzetti et al. (2000) is 10.3. We want to emphasize that the definition of $f_{\rm esc}^{\rm Ly\alpha}$ we are using for high-redshift galaxies includes any effect that would decrease the number of observed Lyα photons with respect to the number expected from the SFR derived from the UV continuum level. The leaking of ionizing photons, as we will discuss later, would therefore imply an $f_{\rm esc}^{\rm Ly\alpha}$ value below unity, even if 100% of the Lyα photons effectively produced in the galaxy are able to escape without being affected by resonant trapping or destruction by dust.

2.2. Limits of Integration

The goal of this study is to determine the total volumetric escape fraction of a given volume, and ideally would include the very faintest systems. In practice, this would require the integration of the LFs down to zero, which, depending on the observational limits of a given survey and the redshift-dependent values of both $L_\star$ and α, may include large extrapolations (or may even be divergent). It is therefore vital that our study employs lower integration limits that are (1) self-consistent between the populations, (2) include a sufficiently meaningful fraction of $\rho_{\rm L}$, and (3) are not dominated by overextrapolation and uncertainties in the faint-end slope.

At $z = 2$, 3, and >4, several studies of the $\rho_{\rm L,UV}$ have been published, and here we adopt those of Reddy et al. (2008) and Bouwens et al. (2009), respectively. Both perform integrations down to $0.04 L_{\star,\rm UV}^{z=3}$ and integrate to the same numerical lower

[7] LFs are typically parameterized by the Schechter (1976) function: $\Phi(L) \cdot dL = \phi_\star \cdot (L/L_\star)^\alpha \cdot \exp(L/L_\star) \cdot dL/L_\star$.

limit at all redshifts. The lower limit is, of course, somewhat arbitrary, but is designed to find a reasonable medium between including a large fraction of the total luminosity/SFR density, and preventing (possible over–) extrapolation by integrating to zero. In this sense, it reflects the observational limits of the UV surveys.

Admitting that this number is somewhat arbitrary, we adopt the same approach and use $0.04L_{\star}^{z=3} - \infty$ as the range for all of the integrations of the UV LF. For $M_{\star}^{z=3} = -21.0$ (AB), the corresponding lower luminosity limit is 4.36×10^{27} erg s^{-1} Hz^{-1} (unobscured SFR $= 0.6\ M_{\odot}$ yr^{-1}). By adopting this limit, our results can easily be cross-checked against the available literature. At redshift 3 for the UV LF of Reddy et al. (2008), this range incorporates 70% of the luminosity, compared to an infinite integration under the LF.

Deciding upon a lower limit for the Hα LF is trickier, since it is difficult to know if we are extracting comparable samples of galaxies. There is no available $z = 3$ Hα LF, but if we adopt that compiled at $z = 2.2$ in Hayes et al. (2010b), and set the lower limit to 0.04 $L_{\star}$, we obtain 4.6×10^{41} erg s^{-1}. This corresponds to much higher unobscured SFR than the lower UV limit at 3.5 $M_{\odot}$ yr^{-1}. However, the UV and Hα-selection functions naturally recover galaxies of different dust contents; if we translate these limits to "true" SFRs for the respective samples, we obtain limits of 2.6 and 6.0 $M_{\odot}$ yr^{-1} for the UV and Hα, respectively. These limits differ by a factor of over two in SFR, but still are not able to account for the differing populations of galaxies that survive the respective selection functions; were the dustier galaxies that are selected by Hα able to enter the UV-selected catalogs, the increased average dust content would bring these values even closer together. We also argue that to some extent, the overall shape of the UV and Hα LFs must be governed by the same physical processes and, regardless of the exact dust content, selecting galaxies brighter than a certain fraction of the characteristic luminosity should recover objects with similar underlying SFRs. Ultimately this argument is backed up in Section 2.3 when we find very similar UV- and Hα-derived SFRs in the local universe, and by the very similar SFRDs derived by the two tracers in Reddy et al. (2008) and Hayes et al. (2010b). Naturally, by cutting both LFs at the same fraction of $L_{\star}$, we recover similar fractions of the luminosity density compared with integration from zero (70%).

For Lyα, the situation is more complicated still: cutting at the same intrinsic SFR would mean that we do not include Lyα emission at lower luminosities. This is now not simply a matter of dust attenuation, but also includes radiation transport effects. Since we expect the line to be systematically weakened, applying a cut at the corresponding SFR to that of Hα or the UV would cause us to miss much of this light. The best way to proceed, therefore, is to adopt the same philosophy as above, and adopt 0.04 $L_{\star,\mathrm{Ly}\alpha}^{z=3}$. By selecting the LF of Gronwall et al. (2007), we obtain a lower limit of 1.75×10^{41} erg s^{-1}. Should $f_{\mathrm{esc}}^{\mathrm{Ly}\alpha} = 1$, this would correspond to an SFR of just 0.15 $M_{\odot}$ yr^{-1}. However, in Hayes et al. (2010a) we determined a volumetric $f_{\mathrm{esc}}^{\mathrm{Ly}\alpha}$ of just 5%, and scaling this SFR up by a factor of 20 brings it to 2.9 $M_{\odot}$ yr^{-1}, almost perfectly into line with the UV-derived 2.6 $M_{\odot}$ yr^{-1} discussed above. Naturally, this integration from 0.04 $L_{\star}$ again includes ≈70% of the total luminosity density (compared with integrating from zero).

In summary, selecting the optimal integration limits is a non-trivial process; yet we argue that by adopting these limits we should be selecting very similar samples of galaxies, at least with respect to their unobscured SFR. The lower limits are 4.36×10^{27} erg s^{-1} Hz^{-1} (UV), 4.6×10^{41} erg s^{-1} (Hα), and 1.75×10^{41} erg s^{-1} (Lyα). We have ensured that these limits include the bulk of the luminosity density but are not dominated in uncertainty by extrapolation in the faint end, although we have also confirmed that integration to zero in fact has only very minor effects on the final measurements of $f_{\mathrm{esc}}^{\mathrm{Ly}\alpha}$.

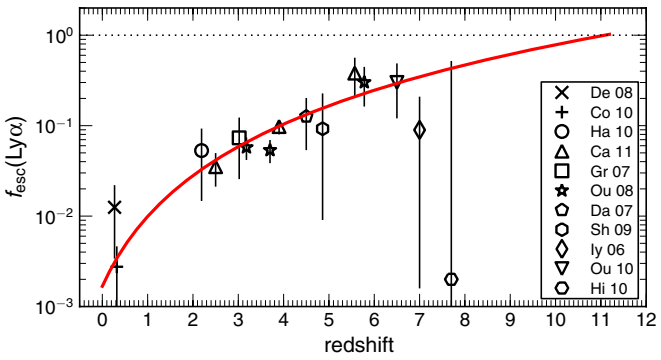

Figure 1. Redshift evolution of $f_{\mathrm{esc}}^{\mathrm{Ly}\alpha}$. Publication codes are listed in the footnote of Table 1. Points at $z = 3.1$ and 5.7 that would overlap have been artificially shifted by $\Delta z = 0.08$ for clarity. The point from Hibon et al. (2010) takes, according to our definition, a value of zero. It is therefore displayed at a value of 0.002 to permit visualization on a logged axis. The solid red line shows the best fitting power law to points between redshifts 0 and 6, which takes an index of $\xi = 2.6$ and is clearly a good representation of the observed points over this redshift range. It intersects with the $f_{\mathrm{esc}}^{\mathrm{Ly}\alpha} = 1$ line (dotted) at redshift 11.1.
(A color version of this figure is available in the online journal.)

2.3. Compilation of the Samples

All of the assembled data and the derived $f_{\mathrm{esc}}^{\mathrm{Ly}\alpha}$ measurements are summarized in Table 1 and Figure 1. The measurements of E_{B-V} relevant to each of the Hα or UV measurements are derived from data in the same publication as the Hα or UV LF data themselves (with one exception, which is discussed in the following paragraph). In this subsection, we provide the necessary motivation for our choices and comments on the various samples.

No instrumentation can perform a Lyα-selected survey in the very nearby universe; so we begin at $z \approx 0.2$–0.4 with the Lyα LFs presented in both Deharveng et al. (2008) and Cowie et al. (2010). At these redshifts Hα LFs are available, and therefore we proceed using Equation (2). We adopt the Hα LF of Tresse & Maddox (1998), and correct it for dust attenuation by applying the one magnitude of extinction that is representative of local Hα-selected galaxies (Kennicutt 1992). For security and consistency with higher redshift measurements, we also examine the $z = 0.3$ UV LFs of Arnouts et al. (2005), which we correct for dust using the method of Meurer et al. (1999) and the β slope measured by Schiminovich et al. (2005) in the same sample as Arnouts et al. (2005), finding extremely consistent numbers.

Beyond the very nearby universe, no further Lyα information is available before $z = 2$, where we adopt our own measurement of $f_{\mathrm{esc}}^{\mathrm{Ly}\alpha} = 5.3\% \pm 3.8\%$ (Hayes et al. 2010a), based upon Hα and individually estimated E_{B-V}.

It is already at this juncture in redshift that we lose the possibility of using Hα, and therefore we proceed using published UV LFs and Equation (3). Our next step is to take the Lyα LF of Cassata et al. (2011; $\langle z \rangle = 2.5$) which we contrast against

Table 1
Lyα Escape Fractions with Redshift

Lyα Quantities			Intrinsic Quantities				Derived Results	
z	Reference	$\dot{\rho}_\star$	z	Reference	E_{B-V}	$\dot{\rho}_\star$	$f_{\rm esc}^{\rm Ly\alpha}$[%]	Comment
(1)	(2)	(3)	(4)	(5)	(6)	(7)	(8)	(9)
Estimates based upon Lyα and Hα LFs.								
0.2–0.35	De 08	$(3.79 \pm 1.69) \times 10^{-4}$	0.2–0.35	TM 98	0.33	(0.0303 ± 0.017)	(1.25 ± 0.90)	1 mag at Hα
0.2–0.4	Co 10	$(8.33 \pm 2.60) \times 10^{-5}$	0.2–0.35	TM 98	0.33	(0.0303 ± 0.017)	(0.275 ± 0.18)	1 mag at Hα
2.2	Ha 10	···	2.2	Ha 10	0.22	···	(5.3 ± 3.8)	Multi dimensional M.C.
Estimates based upon Lyα and UV LFs								
2.5	Ca 11	$(7.08 \pm 0.81) \times 10^{-3}$	⟨2.3⟩	Re 08	0.15	(0.201 ± 0.022)	(3.51 ± 0.56)	
3.1	Gr 07	$(8.50 \pm 5.32) \times 10^{-3}$	⟨3.05⟩	Re 08	0.14	(0.116 ± 0.017)	(7.33 ± 4.71)	
3.1	Ou 08	$(5.54 \pm 2.91) \times 10^{-3}$	⟨3.05⟩	Re 08	0.14	(0.116 ± 0.017)	(4.78 ± 2.61)	
3.7	Ou 08	$(4.78 \pm 1.14) \times 10^{-3}$	⟨3.8⟩	Bo 09	0.14	(0.089 ± 0.011)	(5.36 ± 1.43)	
3.8	Ca 11	$(8.71 \pm 1.00) \times 10^{-3}$	⟨3.8⟩	Bo 09	0.14	(0.089 ± 0.011)	(9.77 ± 1.64)	
4.5	Da 07	$(3.22 \pm 1.25) \times 10^{-3}$	⟨4.7⟩	Ou 04	0.075	(0.025 ± 0.011)	(12.6 ± 7.17)	
4.86	Sh 09	$(2.35 \pm 3.17) \times 10^{-3}$	⟨4.7⟩	Ou 04	0.075	(0.025 ± 0.011)	(9.24 ± 13.0)	
5.65	Ca 11	$(8.53 \pm 3.44) \times 10^{-3}$	⟨5.9⟩	Bo 09	0.029	(0.022 ± 0.005)	(38.1 ± 17.2)	
5.7	Ou 08	$(6.76 \pm 4.77) \times 10^{-3}$	⟨5.9⟩	Bo 09	0.029	(0.022 ± 0.005)	(30.2 ± 22.2)	
6.6	Ou 10	$(4.73 \pm 1.24) \times 10^{-3}$	6.5	Bo 07	0.012	(0.016 ± 0.008)	(30.0 ± 17.8)	UV Interpolated
7.0	Iy 06	$(1.07 \pm 1.16) \times 10^{-3}$	7.0	Bo 09	0.010	(0.012 ± 0.008)	(8.96 ± 11.5)	UV Interpolated
7.7	Hi 10	$(0^{+88.5}_{-0}) \times 10^{-3}$	7.7	Bo 10	0.0	(0.005 ± 0.002)	$(0^{+50.6}_{-0})$	UV Interpolated

Notes. For the Hα-based estimates, we use the integrated luminosity densities directly; SFRD measurements are presented just for homogeneity with the UV estimates. $\dot{\rho}_\star$ units are $M_\odot$ yr^{-1} Mpc^{-3} and E_{B-V} is in magnitudes. The references are expanded as: Bo 09 = Bouwens et al. (2009); Ca 11 = Cassata et al. (2011); Co 10 = Cowie et al. (2010); Da 07 = Dawson et al. (2007); De 08 = Deharveng et al. (2008); Gr 07 = Gronwall et al. (2007); Ha 10 = Hayes et al. (2010a); Hi 09 = Hibon et al. (2010); Iy 08 = Iye et al. (2006); Ou 04 = Ouchi et al. (2004); Ou 08 = Ouchi et al. (2008); Ou 10 = Ouchi et al. (2010); Sh 09 = Shioya et al. (2009); Re 08 = Reddy et al. (2008); TM 98 = Tresse & Maddox (1998). References for E_{B-V} measurements are the same as for the intrinsic SFRD (i.e., that listed in the fifth column) with the exception of the $\langle z \rangle = 0.3$ points in which E_{B-V} is adopted from Kennicutt (1992).

the dust-corrected $\rho_{\rm L,UV}$ of Reddy et al. (2008, $\langle z \rangle = 2.3$). For this, and all subsequent points from Cassata et al. (2011), we adopt the values of $L_\star$ that are uncorrected for IGM attenuation. It is re-assuring that the measurements at $z = 2.2$ and $z \approx 2.5$ (which are based upon Hα and UV, respectively) give very consistent numbers. Furthermore, in a very recent submission (Blanc et al. 2010), an additional Lyα LF has been presented at $1.9 < z < 2.8$, the integrated Lyα luminosity density which differs from our own result by ≈25%.

We then continue with the Reddy et al. (2008) UV data at $\langle z \rangle = 3.05$, which we use to compute $f_{\rm esc}^{\rm Ly\alpha}$ for the $z = 3.1$ Lyα samples of Gronwall et al. (2007) and Ouchi et al. (2008).

At $z \sim 4$, we have available Lyα LFs from Ouchi et al. (2008, $z = 3.7$) and Cassata et al. (2011, $z = 3.9$), and UV LFs from Bouwens et al. (2007, $\langle z \rangle = 3.8$). We also use the $z = 4.5$ and 4.86 Lyα LF points from Dawson et al. (2007) and Shioya et al. (2009), which we normalize by the dust-corrected UV point at $z = 4.7$ from Ouchi et al. (2004).

The next redshift to examine is the popular $z \approx 5.7$ Lyα window. Here, we adopt the UV data point from the *i*-dropout sample of Bouwens et al. (2007, $\langle z \rangle = 5.9$), and the Lyα LF Ouchi et al. (2008, $\langle z \rangle = 5.7$), which is in good agreement with those of Shimasaku et al. (2006), Ajiki et al. (2006), and Tapken et al. (2006). We also add the highest redshift LF from Cassata et al. (2011) at $\langle z \rangle = 5.65$.

Finally, we assemble a few $z > 6$ samples. We adopt the $z = 6.5$ point from Ouchi et al. (2010, which includes the sample of Kashikawa et al. 2006), and the measurement of Iye et al. (2006) at $z = 7.0$, which has also been compiled in Ota et al. (2008). Here, we adopt Bouwens et al. (2010b) UV measurement at $\langle z \rangle = 6.8$ for comparison. It should be noted that at this redshift the dust-corrected and uncorrected measurements of Bouwens et al. (2010b) converge. We adopt the most optimistic estimate at $z = 7.7$ from Hibon et al. (2010), for which we interpolate between the Bouwens et al. (2010b) at $z = 6.8$ and 8.2 UV data points. Hibon et al. (2010) present Schechter parameters for four Lyα LFs, based upon various assumptions about the rate of contamination by lower redshift galaxies. By assuming all of their candidates are real (their sample *a*), we find a Lyα escape fraction of $(33.5^{+50.6}_{-33.5})$%. We also briefly examine their subsample *b*, in which only four of the seven objects are real. For all of their subsamples, the numbers are insufficient to provide meaningful errors on the luminosity density and by our standard error procedure we derive $f_{\rm esc}^{\rm Ly\alpha} = (22.2^{+1707}_{-22.2})$%. Furthermore, it should be noted that in the Hibon et al. (2010) sample, the lower limits obtained on the Lyα equivalent width are in the range 6–15 Å, with their continuum-detected object showing $W_{\rm Ly\alpha} = 13$ Å. Thus, at an acceptable confidence limit, none of their seven objects would actually survive the canonical $W_{\rm Ly\alpha}$ cut of 20 Å that is typically employed in narrowband surveys. Including these data is therefore not straightforward, but in order to treat them as consistently as possible with the lower redshift points, we have to set the $z \approx 7.7$ Lyα escape fraction to zero, but adopted a characteristic error of 50.6% as derived from their most optimistic sample. We note that this limit is likely extremely high.

All of our measurements of $f_{\rm esc}^{\rm Ly\alpha}$ are listed in Table 1 and shown graphically in Figure 1, which is the main result of this paper.

2.4. Consistency (and Inconsistency) Between Groups

It should always be borne in mind that we are compiling results from different survey teams, who may adopt different techniques for data reduction and photometry, derivation of the LFs, and incompleteness corrections. For example, Malhotra & Rhoads (2004) find reasonable agreement at $z \approx 5.7$ between the narrowband-selected Lyα LFs of Rhoads & Malhotra (2001)

and Ajiki et al. (2004), and the lensing-based survey of Santos et al. (2004). However, the $z = 5.7$ LF of Shimasaku et al. (2006), on which the study of Kashikawa et al. (2006) is based (see Section 5.2), find a strong disagreement at the faint end between their own LF and the compilation of Malhotra & Rhoads (2004). As commented by Shimasaku et al. (2006), the likely cause for this discrepancy lies in (1) the lack of incompleteness corrections, which are unmentioned in any of the 2004 articles, (2) the differences in equivalent-width-based selection criteria, and (3) the large cosmic variance which Ouchi et al. (2008) noted can be of factors of ≈2 in fields as large as 1 deg^2. Our results are sensitive to all of these considerations.

It is only now that sufficiently large samples of Lyα-emitting galaxies are presented in the literature for this study to be undertaken, and we are fortunate that a good fraction of our data must contain internal self-consistency. For example, three of our data points (at $z = 3.1$, 3.7, and 5.7) are drawn from a single paper (Ouchi et al. 2008) in which the methodologies must be internally consistent, and the basic trend can be seen in these data alone. A fourth point at $z = 6.6$ comes from Ouchi et al. (2010) where similar self-consistency is to be expected. In the same fashion, three further points are taken from Cassata et al. (2011) where internally the same methodology must have been adopted at each redshift. It is certainly encouraging that, for example at $z = 5.7$ the measurements of $f_{\rm esc}^{{\rm Ly}\alpha}$ based upon Cassata et al. (2011) and Ouchi et al. (2008) are practically indistinguishable, despite the fact that they are based upon completely different methods: blind spectroscopy and narrowband imaging, respectively. The $z = 2.2$ and 2.5 points of Cassata et al. (2011) and Hayes et al. (2010a) are similarly indistinguishable (and also robust against the same fundamental methodological difference of blind spectroscopy versus narrowband imaging), as are the $z = 3.1$ points of Ouchi et al. (2008) and Gronwall et al. (2007), both based on narrowband imaging.

Any study of the galaxy population benefits from targeting spatially disconnected, independent pointings in order to beat down cosmic variance. By adopting the studies of various authors pointed all over the extragalactic sky, this study is able to benefit from the inclusion of a large number of independent fields.

3. GENERAL RESULTS

3.1. The Evolution of $f_{\rm esc}^{{\rm Ly}\alpha}$

Figure 1 reveals a general and significant trend for $f_{\rm esc}^{{\rm Ly}\alpha}$ to increase with increasing redshift. Beginning in the very local universe we see $f_{\rm esc}^{{\rm Ly}\alpha} \sim 0.01$ or lower for nearby star-forming objects. This increases to around ≈5%–10% by redshift of ≈3–4, and further to ≈30%–40% by redshift 6. In order to quantify this trend we fit an analytical function to these data points, choosing a power law of the form $f_{\rm esc}^{{\rm Ly}\alpha}(z) = C \times (1+z)^{\xi}$—we obtain coefficients of $C = (1.67^{+0.53}_{-0.24}) \times 10^{-3}$; $\xi = (2.57^{+0.19}_{-0.12})$. Note that we do not include any $z > 6$ points in our fit since previous studies suggest that it is around this redshift that an appreciable fraction of the intergalactic hydrogen becomes neutral, and may in principle affect the Lyα LF. For more discussion on this see Section 5.2. To insure that the fit is not biased by the presence of two $z \approx 0.3$ points that lie around 8 Gyr from $z \approx 2$, we repeat the fit after excluding these points, finding $C = (4.79^{+5.68}_{-0.69}) \times 10^{-4}$; $\xi = (3.38^{+0.10}_{-0.37})$. Clearly, the fit is affected by these points, but their exclusion actually results in a more rapid evolution with redshift.

The apparent trend begins to break beyond redshift 6, but it is initially very slow. Over the redshift interval from 5.7 to 6.5, $f_{\rm esc}^{{\rm Ly}\alpha}$ stabilizes, but decreases again to just ≈10% at $z = 7$. The redshift 7 point from Iye et al. (2006) is confirmed, whereas none of the sample of redshift 7.7 candidates from Hibon et al. (2010) have confirmations by spectroscopy, and this upper error bar must be regarded as an optimistic upper limit.

Finally, we perform a simple experiment with the best-fit relationship to the $f_{\rm esc}^{{\rm Ly}\alpha}$–$z$ trend, and extrapolate to estimate the redshift at which $f_{\rm esc}^{{\rm Ly}\alpha}$ reaches unity. This would carry the implication that the ISM of the average galaxy has become effectively devoid of dust, and since dust is a byproduct of the star formation process, must also correspond to a time of approximately primeval star formation. It is interesting, therefore, that we find $f_{\rm esc}^{{\rm Ly}\alpha} = 1$ at $z = 11.1^{+0.8}_{-0.6}$, which is consistent with the redshift of the instantaneous reionization of the universe based upon *Wilkinson Microwave Anisotropy Probe* data ($z = 11 \pm 1.4$; Dunkley et al. 2009).

3.2. Comparison with the Literature

Naturally, this is not the first time that $f_{\rm esc}^{{\rm Ly}\alpha}$ has been estimated and several other studies based on a wide array of methods have attempted to pin down the same quantity at different redshifts. For example, at redshifts of 5.7 and 6.5, we compute $f_{\rm esc}^{{\rm Ly}\alpha}$ of around 40% and 30%, respectively. Based upon the fitting of spectral energy distributions (SEDs) to stacked broadband fluxes, Ono et al. (2010) estimate $f_{\rm esc}^{{\rm Ly}\alpha} = (36^{+68}_{-35})\%$ and $(4^{+180}_{-3.8})\%$ at the same redshifts. Although derived from an interesting approach, the uncertainties are still too large to provide a useful comparison.

Like us, Nagamine et al. (2010) compared observed Lyα LFs (Ouchi et al. 2008, in this case, which we also use) with intrinsic estimates, having derived this intrinsic LF from smoothed particle hydrodynamical (SPH) models of galaxy formation. They adopt two methods of scaling the intrinsic to the observed LFs, the first of which they call "escape fraction," which is a scaling to the data points along the luminosity axis, and assumes all galaxies have the same $f_{\rm esc}^{{\rm Ly}\alpha}$. This method finds $f_{\rm esc}^{{\rm Ly}\alpha} = 10\%$ at $z = 3$, which is certainly consistent with our estimates based on the $z = 3.1$ LF of Gronwall et al. (2007) and similar to but slightly higher than our estimate based on Ouchi et al. (2008). At $z = 6$, however, Nagamine et al. (2010) require an escape fraction of just 15% which is lower than our estimates of 30%–40%, and discrepant with our estimates at around the 2σ level. Nagamine et al. (2010) also test a "duty-cycle" scenario (an LF scaling along the Φ axis) in which only a fraction of the SPH galaxies are "on" as Lyα emitters, but emit 100% of their Lyα photons. Note that in these two extreme scenarios, there is no requirement for the integral over the scaled LF to be equivalent. Nagamine et al. (2010) present duty cycles of 0.07 and 0.2 at $z = 3$ and 6, respectively. However, before they compute these scalings the observed LFs are shifted along the luminosity axis by IGM attenuation factors of 0.82 ($z = 3$) and 0.52 ($z = 6$). This re-scaling needs to be removed before making a comparison with our estimate, and in the duty-cycle scenario the volumetric escape fractions that one would infer from the study of Nagamine et al. (2010) are 6% at $z = 3$ and 10% at $z = 6$. Again this agrees very well with our measurement at $z \approx 3$, but compared with our estimates at $z = 6$ is an underestimate of around the same magnitude as their escape fraction method.

In contrast, using similar SPH galaxy formation models but modified prescriptions for Lyα production and transmission, as well as a different reionization history, Dayal et al. (2009) find Lyα escape fractions of 30% at both $z = 5.7$ and 6.5, which corresponds exactly with our measurements. Similar values of $f_{\rm esc}^{\rm Ly\alpha} \sim 23\%$–$33\%$ have also been obtained in the followup work of Dayal et al. (2010), although they also include an IGM transmission of $T_\alpha = 0.48$. Throughout this paper we have made sure not to apply any IGM correction, since the value of T_α remains poorly constrained, even theoretically, and from an observational perspective there is no strong evidence for exactly how close the IGM comes to a narrow Lyα line. As with the Madau (1995) prescription, it is likely that this IGM transmission is too low when considering lines that are systematically redshifted by the kinematics of the ISM, which would drive up these theoretical estimates of the Lyα escape fraction.

Adopting a similar method of LF scaling by luminosity, Le Delliou et al. (2005) found that an escape fraction of 2% was sufficient to match observed Lyα LFs with their predictions based upon semi-analytical models between $z = 2$ and 6, with the same machinery able to predict the clustering properties of Lyα emitters (Orsi et al. 2008). This is at the lower end of being consistent with our $z = 3$ measurements, and should the same escape fraction hold at $z = 0.3$, would also be consistent with our estimates in the nearby universe. However, the Le Delliou et al. (2005) escape fraction is highly inconsistent with our estimates at higher redshift. These semi-analytical models, using the prescription of Baugh et al. (2005), categorized star formation as occurring in two discrete modes, with a normal Salpeter IMF ($\alpha = -1.35$) assigned to quiescent star formation and a flat IMF ($\alpha = 0$) for bursting systems. This flat IMF increases the ionizing photon production at a given SFR by a factor of 10 and was implemented as a requirement in order to reproduce the population of submillimeter-selected galaxies at $z > 2$. However, as noted by Le Delliou et al. (2006), the fraction of total star formation that occurs in bursts increases from 5% at $z = 0$ to over 80% at $z = 6$, and thus their model implies that by the $z = 5.7$ points; effectively all stars are formed in environments where ionizing photons are greatly overproduced compared with the present day. Should this requirement of the flat IMF be removed and the Salpeter IMF applied throughout, the intrinsic rate of production of ionizing photons would be decreased by a factor of three at $z = 3.1$ where the star formation is shared evenly between bursting and quiescent systems. This would bring the $f_{\rm esc}^{\rm Ly\alpha}$ estimate to 11% at this redshift. At $z = 6$, $f_{\rm esc}^{\rm Ly\alpha} = 16\%$ would be found by replacing the flat IMF with the Salpeter IMF. These numbers are indeed very similar to the SPH models of Nagamine et al. (2010), but inconsistent with those of Dayal et al. (2009) and our own estimates based upon observation. It is interesting to point out, however, that the IMF assumption has little effect on the $z \approx 0.3$ points where, in their model, the quiescent mode of star formation dominates.

3.3. Possible Physical Explanations

The evolution in measured $f_{\rm esc}^{\rm Ly\alpha}$ is substantial, covering approximately two orders of magnitude, and no doubt holds vital information about the physical nature of galaxies at various cosmic epochs. As we will show in Section 5, the most likely explanation for this evolution is the decrease of the average dust content of galaxies. However, from a physical perspective many effects may enter. For example, galaxies may also contain less neutral hydrogen to scatter photons, show faster outflows, or become more clumpy. The inferred increase may alternatively be mimicked by galaxies becoming younger on average, having low and decreasing metallicities, or forming stars with IMFs that become more biased in favor of massive, ionizing stars. On the other hand, the scattering of Lyα photons by a neutral IGM and the general leakage of ionizing photons (Lyman continuum; LyC) are expected to increase with increasing redshift, and would both serve to lower the perceived Lyα escape fraction (although the "true" $f_{\rm esc}^{\rm Ly\alpha}$ of galaxies, i.e., before the IGM, would not be affected).

Regrettably, we are not able to measure any of these quantities directly from this compilation of data. We have, however, assembled data that show a number of trends with redshift: the Lyα and UV luminosity densities and the dust contents. These we have combined to show how $f_{\rm esc}^{\rm Ly\alpha}$ evolves; yet in order to extract the maximum of information from these, we need to examine another possible trend: how $f_{\rm esc}^{\rm Ly\alpha}$ correlates with the dust content. Thus, we delay a detailed discussion of what drives the $f_{\rm esc}^{\rm Ly\alpha}$–$z$ trend until Section 5 and now proceed to discuss the effects of radiation transport and dust absorption.

4. THE Lyα ESCAPE FRACTION AND ITS DEPENDENCES

That Lyα photons undergo a complex radiation transport, in which a large number of parameters enter, is well known but poorly understood from an empirical angle. Transport is thought to be affected by dust content (Atek et al. 2008, 2009; Hayes et al. 2010a), dust geometry (Scarlata et al. 2009), H I content and kinematics (Kunth et al. 1998; Mas-Hesse et al. 2003; Shapley et al. 2003; Tapken et al. 2007), and geometry/neutral-ionized gas topology (Neufeld 1991; Giavalisco et al. 1996; Hansen & Oh 2006; Finkelstein et al. 2008, 2009). Unfortunately, H I masses remain impossible to be measured directly beyond the very local universe. Kinematic measurements of the neutral ISM can be obtained at high redshift, but require deep absorption line spectroscopy against the vanishing continuum of Lyα-selected galaxies and thus are prohibitively expensive for large samples of individual galaxies. We are therefore effectively limited, when targeting statistically meaningful samples, to examining Lyα emission against the dust content, and have to infer information about the remaining quantities by secondary analysis.

Significant anti-correlations between $f_{\rm esc}^{\rm Ly\alpha}$ and E_{B-V} have been presented in four recent papers, all of which invoke different selection functions and employ different methods of analysis. First, Verhamme et al. (2008) used radiation transport modeling of spectrally resolved Lyα features in a sample of Lyman Break Galaxies (LBGs) between redshifts 2.8 and 5 to estimate both dust attenuation and $f_{\rm esc}^{\rm Ly\alpha}$. Based upon the Balmer line ratio (Hα/Hβ), Atek et al. (2009) computed $f_{\rm esc}^{\rm Ly\alpha}$ and nebular reddenings based upon purely nebular physics in a sample of nearby Lyα-selected galaxies. Were Hα and Hβ observations available in the distant universe, this method would be the ideal one by which to proceed. More recently, Kornei et al. (2010) performed a similar experiment in a sample of redshift $\sim$3 Lyα-emitting LBGs, in which dust attenuation and intrinsic Lyα luminosities were estimated from modeling of the SED. Finally, in a sample of redshift 2 Lyα- and Hα-selected galaxies, we also used SED modeling to estimate E_{B-V}, but estimated the intrinsic Lyα production from the dust-corrected Hα luminosity (Hayes et al. 2010a).

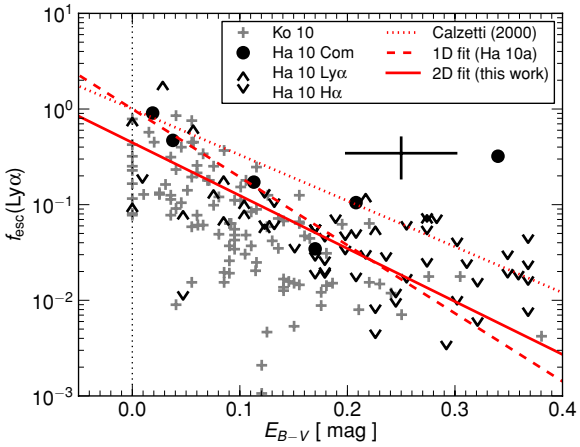

Figure 2. Literature compilation of $f_{esc}^{Ly\alpha}$ vs. E_{B-V}. The codings in the legend are: Ha 10 = Hayes et al. (2010a) and Ko 10 = Kornei et al. (2010). Solid circles from Hayes et al. (2010a) are six objects for which we have detections in both Lyα and Hα. Caret down markers are Hα emitters that were undetected in Lyα and hence presented as upper limits, while caret up markers are Lyα galaxies for which Hα lies below the detection limit and are presented as lower limits. Error bars are removed from the plot to aid readability, but the average error from the common detections of Hayes et al. (2010a) is shown by the singular black point with error bars. For further information the reader is referred to Figure 3 of Hayes et al. (2010a). The red lines show various conversions between the observed stellar E_{B-V} and $f_{esc}^{Ly\alpha}$. The dotted line shows the standard Calzetti et al. (2000) prescription, the dashed line shows the one-dimensional fit to the data from Hayes et al. (2010a), and the solid line shows a two-dimensional fit described in the text.

(A color version of this figure is available in the online journal.)

In Figure 2, we show a compilation of the $f_{esc}^{Ly\alpha}$ and E_{B-V} points from Kornei et al. (2010) and Hayes et al. (2010a). Here, we adopt only these two data sets since they involve similar computations of E_{B-V}, but include Lyα, Hα, and UV selection and should be broadly representative of the general galaxy populations under consideration in this paper. These two studies both perform full SED fits, but use them in different ways, with Kornei et al. (2010) requiring the intrinsic ionizing photon budget to estimate $f_{esc}^{Ly\alpha}$ and Hayes et al. (2010a) using only the E_{B-V} estimate to correct Hα for the dust attenuation. Thus, the Kornei et al. (2010) points are in principle expected to be more sensitive to the standard set of assumptions in population synthesis (IMF, stellar atmosphere models, etc.). However, a substantial overlap between the two populations is clear in Figure 2, with the two populations occupying a very similar region of the $f_{esc}^{Ly\alpha}$–E_{B-V} plane (the fact that we find more galaxies at higher E_{B-V} is due to the fact that we find redder galaxies by Hα selection than is possible using the UV-biased Lyman-break criterion).

The dotted line shows the dust attenuation prescription of Calzetti et al. (2000) which should be valid in the case of no Lyα scattering and a simple dust screen. This line is described by $f_{esc}^{Ly\alpha} = 10^{-0.4 \cdot E_{B-V} \cdot k_{1216}}$, where $k_{1216} = 12$. Very few points lie above this line and all are likely placed there by statistical scatter. Indeed, this line sets an approximate upper limit to the data points, which extend in the direction of lower $f_{esc}^{Ly\alpha}$ due to radiation transport effects increasing the effective dust optical depth seen by Lyα.

In attempts to quantify the effects of resonance scattering and dust absorption, the studies of Verhamme et al. (2008), Atek et al. (2009), and Hayes et al. (2010a) all fit linear relationships to the data points on the $\log(f_{esc}^{Ly\alpha})$–E_{B-V} plane, assuming no a priori information about the dust. These studies all used a functional form of $f_{esc}^{Ly\alpha} = 10^{-0.4 \cdot E_{B-V} \cdot k_{Ly\alpha}}$, where $k_{Ly\alpha}$ (the single free parameter of the fit) is an effective extinction coefficient for Lyα, and thus includes both scattering and absorption. Both at high-z, the studies of Verhamme et al. (2008) and Hayes et al. (2010a) found effectively the same value of $k_{Ly\alpha} = 17.8$, which runs significantly steeper than the Calzetti et al. (2000) relationship as Lyα photons are preferentially attenuated. This is shown by the dashed line in Figure 2.

These formalisms force the fits to conform to $f_{esc}^{Ly\alpha} = 1$ at $E_{B-V} = 0$, and technically it is true that if there is exactly zero dust, Lyα photons cannot be absorbed by dust. However, the very presence of Lyα photons implies that star formation must be occurring and, after just ~3 Myr of star formation, dust produced in supernovae would be returned to the ISM and the optical color excess ceases to be a good proxy for dust. It is well known that Lyα can be strongly suppressed even when miniscule amounts of dust are present (e.g., Hartmann et al. 1984; Kunth et al. 1994; Thuan & Izotov 1997; Östlin et al. 2009) and, as Figure 2 shows, some galaxies have $f_{esc}^{Ly\alpha} = 10\%$ with no measurable UV attenuation. Indeed, many star-forming galaxies show little or no attenuation in front of their ionizing clusters but substantially attenuated nebular regions. This is the origin of the factor of 2.2 difference between stellar and nebular measurements of E_{B-V} (Calzetti et al. 2000), but at a very low UV stellar attenuation of $E_{B-V} \approx 0$ applying a factor of two is not meaningful and nebular lines in general—and Lyα in particular—may be heavily attenuated. It is unfortunate that at high-z the UV continuum is our only proxy for the dust content as we indeed expect to be surveying redshifts at which the stellar attenuation indeed falls to ~0 (e.g., Bouwens et al. 2009).

To account for these factors, we now proceed to relax the requirement of the fit passing through $(E_{B-V}, f_{esc}^{Ly\alpha})=(0,1)$ and re-fit the combined data sets of Kornei et al. (2010) and Hayes et al. (2010a) using the following expression:

$$f_{esc}^{Ly\alpha} = C_{Ly\alpha} \cdot 10^{-0.4 \cdot E_{B-V} \cdot k_{Ly\alpha}}. \quad (4)$$

This expression takes the same form as the standard dust-screen prescription, with coefficient $k_{Ly\alpha}$, but adds the additional parameter of $C_{Ly\alpha}$, the factor by which $f_{esc}^{Ly\alpha}$ is scaled down. As in Hayes et al. (2010a), we use Schmidt's binned linear regression algorithm (Isobe et al. 1986), since it permits the combination of data points and limits in both directions. For $k_{Ly\alpha}$ we obtain a value of 13.8, which is much more similar to the value of 12.0 obtained from Calzetti et al. (2000) at the wavelength of Lyα. However, we also obtain $C_{Ly\alpha} = 0.445$, indicating that we expect $f_{esc}^{Ly\alpha}$ to be around 50%, even when there is no measurable dust attenuation on the stellar continuum. This is in fact a more plausible scenario, since the effect of scattering by neutral hydrogen is not expected to depend on the dust content itself. This fit is shown by the solid red line in Figure 2. Again the points of Kornei et al. (2010) and Hayes et al. (2010a) are subject to different assumptions that enter the population synthesis. However, for the reasons outlined previously in this subsection and the similarity between the distributions, we do not expect these quantities to be strongly subject to these assumptions.

It is not necessarily straightforward to define a goodness-of-fit measurement to compare the quality of the three fits, given the large number of upper and lower limits in this data set. Thus,

we define our own normalized rms statistic ($\mathrm{rms_n}$) as

$$\mathrm{rms}_n = \sqrt{\frac{1}{N}\sum_i^N \left(\frac{f_i^{\mathrm{meas}} - f_i^{\mathrm{EBV}}}{f_i^{\mathrm{meas}}}\right)^2}, \quad (5)$$

where f_i^{meas} is the ith-measured Lyα escape fraction, f_i^{EBV} is the ith Lyα escape fraction predicted from E_{B-V}, and N is the number of data points. However, in order to treat the limits, we permit a point to contribute to the summation only if that limit is violated. We appreciate that this is a non-standard statistic, but it does enable a quantitative measure of the goodness of fit that is philosophically not too far removed from more commonplace statistics. Adopting the $f_{\mathrm{esc}}^{\mathrm{Ly}\alpha}$–$E_{B-V}$ relations derived from Calzetti et al. (2000), the one parameter fit from Hayes et al. (2010a), and the two parameter fit from this work, we compute rms_n = 1.85, 1.02, and 0.66, respectively.

We have now assembled information about three trends: the observed redshift evolution of $f_{\mathrm{esc}}^{\mathrm{Ly}\alpha}$, the observed redshift evolution of the dust content of galaxies, and the observed relationship between $f_{\mathrm{esc}}^{\mathrm{Ly}\alpha}$ and the dust content. We will next show that we are able to synthesize these points to infer some general trends in the evolution of galaxies.

5. ON THE EVOLUTION OF $f_{\mathrm{esc}}^{\mathrm{Ly}\alpha}$

5.1. Redshifts 0–6: the Upwardly Evolving Escape Fraction and the Properties of Galaxies

5.1.1. The Evolving Dust Content of Galaxies

We showed in the previous section that $f_{\mathrm{esc}}^{\mathrm{Ly}\alpha}$ of individual galaxies is anti-correlated with the measured E_{B-V} (Figure 2). Given that the typical E_{B-V} evolves with redshift (see Table 1), we may indeed expect a positive correlation between $f_{\mathrm{esc}}^{\mathrm{Ly}\alpha}$ and redshift. This is exactly what Figure 1 shows, where it is clear that the Lyα escape fraction increases smoothly and monotonically out to $z \sim 6$. Thus, it appears that this increase in $f_{\mathrm{esc}}^{\mathrm{Ly}\alpha}$ is the result of the dust content of the star-forming galaxy population decreasing with redshift. We now take the measured values of E_{B-V} from the various samples (listed in Table 1), and use them to compute the $f_{\mathrm{esc}}^{\mathrm{Ly}\alpha}$ that would be expected from the three conversions between E_{B-V} and $f_{\mathrm{esc}}^{\mathrm{Ly}\alpha}$ discussed in the previous section (Calzetti et al. 2000; an empirical fit with one free parameter from Hayes et al. 2010a; and an empirical fit with two free parameters from this study). We show the measured escape fractions together with these predictions in Figure 3.

We first discuss the predictions based upon the Calzetti et al. (2000, red dotted line), which is clearly discrepant with the observations at around the 3σ level at every redshift. Obviously, this is to be expected since Lyα photons resonantly scatter and it is unlikely that the dust is distributed in a uniform screen. The one-dimensional fit from Hayes et al. (2010a) offers substantial improvement and is able to describe the observations between redshifts 0 and 4. This reasoning is circular for the redshift 2 points where the $f_{\mathrm{esc}}^{\mathrm{Ly}\alpha}$–$E_{B-V}$ relationship was derived, but we stress the tautology is present only at this redshift. This relationship is not able to explain any of the data points at redshift above 4, where it systematically overpredicts the Lyα escape fraction.

As redshift increases, the dust content of galaxies is clearly shown to change, and could we plot Figure 2 at redshifts higher than 3, we would expect galaxies to cluster successively further toward the upper left corner of the plot. Since the Hayes et al. (2010a) $f_{\mathrm{esc}}^{\mathrm{Ly}\alpha}$–$E_{B-V}$ fit is forced through the (E_{B-V},$f_{\mathrm{esc}}^{\mathrm{Ly}\alpha}$) = (0,1) coordinate and a high value of $k_{\mathrm{Ly}\alpha}$ is found, the predicted escape fraction evolves very quickly with redshift. Indeed, these predictions evolve much faster than the data, as $f_{\mathrm{esc}}^{\mathrm{Ly}\alpha}$ is forced for unphysical reasons toward unity.

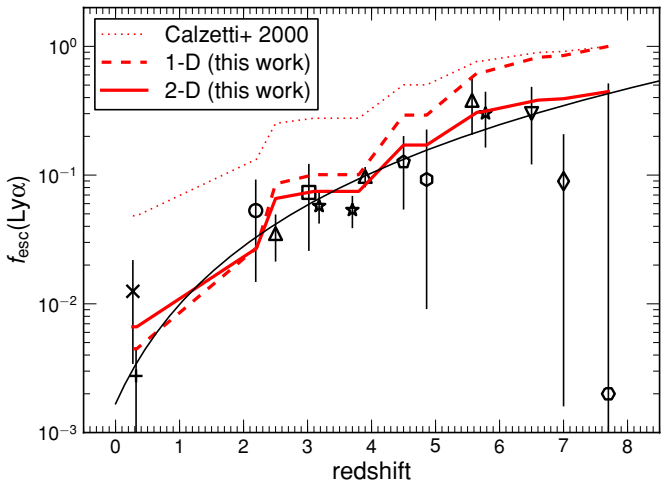

Figure 3. Same as Figure 1, but zoomed onto the relevant region. The red lines show the Lyα escape fractions that would be predicted based upon the values of E_{B-V} that have been measured in the respective Hα and UV samples (listed in Table 1), and using the various conversions between measured E_{B-V} and $f_{\mathrm{esc}}^{\mathrm{Ly}\alpha}$ described in the text. The dotted line represents the dust attenuation law of Calzetti et al. (2000); the dashed line represents the one-dimensional empirical fit to the data of Hayes et al. (2010a); and the solid line represents a two-dimensional fit to the data described in Section 4. Using the two-dimensional fit, a remarkably good agreement is seen between observations and prediction between redshifts 0 and 6.5.

(A color version of this figure is available in the online journal.)

When we introduce the new $f_{\mathrm{esc}}^{\mathrm{Ly}\alpha}$–$E_{B-V}$ fit with two free parameters and allow $C_{\mathrm{Ly}\alpha} \neq 1$, the agreement between the measured and observed Lyα escape fractions is striking: it agrees with essentially every data point, within the error bars, between redshifts 0 and 6.6. We should point out that it is not clear that the use of the average E_{B-V} for a sample should by necessity reproduce the volumetric escape fraction. Due to variations of the dust contents and ISM of individual galaxies, and the associated impact upon the transfer of Lyα and the selection of galaxies, it is plausible that the average $f_{\mathrm{esc}}^{\mathrm{Ly}\alpha}$ could have been skewed substantially from the data points. Indeed, close examination of the $f_{\mathrm{esc}}^{\mathrm{Ly}\alpha}$–$E_{B-V}$ relationship ($C_{\mathrm{Ly}\alpha}$ = 1; $k_{\mathrm{Ly}\alpha}$=17.8) from Hayes et al. (2010a) reveals that it does not perfectly intersect the center of the $f_{\mathrm{esc}}^{\mathrm{Ly}\alpha}$ data point (z = 2.2 point in Figure 3) from the same survey, despite $f_{\mathrm{esc}}^{\mathrm{Ly}\alpha}$, average E_{B-V}, and the coefficients of the $f_{\mathrm{esc}}^{\mathrm{Ly}\alpha}$–$E_{B-V}$ relationship all having been derived entirely from this one data set. This most likely results from the weighting across the population from which the average E_{B-V} is computed (the representative E_{B-V} is not an average weighted by the intrinsic Lyα luminosity), exactly the effect under discussion. However, the fact that such tight agreement is seen between the observational estimates and those derived from our fit suggests that such a bias in the selection of the populations is not at play here.

Again we stress that the relationship we derived between $f_{\mathrm{esc}}^{\mathrm{Ly}\alpha}$ and E_{B-V} in Section 4 includes the effects of resonance

scattering, and thus in some manner the neutral gas content, its kinematics, and relative geometry all enter the relationship, which holds even when the measured optical color excess on the stellar continuum is zero. There is no reason to assume that these quantities are constant with redshift and we could, for example, envisage situations where the gas content, feedback properties, or clumpiness evolve and thereby change $k_{\mathrm{Ly}\alpha}$ or $C_{\mathrm{Ly}\alpha}$. However, the tight agreement between our observed $f_{\mathrm{esc}}^{\mathrm{Ly}\alpha}$ values and those computed from the $f_{\mathrm{esc}}^{\mathrm{Ly}\alpha}$-$E_{B-V}$ relationship provides no evidence for the evolution of these properties (at least if the gas content does change it does not take part in the Lyα- scattering process). The evolution of $f_{\mathrm{esc}}^{\mathrm{Ly}\alpha}$ across almost the entire observable universe can be explained cleanly within the confines of this simple model, as mainly due to a dust content that evolves with redshift.

5.1.2. Other Effects

We need to interpret an increase in the global $f_{\mathrm{esc}}^{\mathrm{Ly}\alpha}$ of galaxies by a factor of $\sim$4 between $z = 2$ and 6, and naturally if something were to alter the intrinsic Lyα/UV ratio of galaxies by this factor, the evolution in $f_{\mathrm{esc}}^{\mathrm{Ly}\alpha}$ could be mimicked.

For example, there is evidence that the $W_{\mathrm{Ly}\alpha}$ distribution of galaxies changes with increasing redshift: high-$W_{\mathrm{Ly}\alpha}$ objects become relatively more abundant (e.g., Gronwall et al. 2007; cf. Shimasaku et al. 2006; also Ouchi et al. 2008), and thus pure selection may explain the trend. However, the $W_{\mathrm{Ly}\alpha}$ distributions at $z = 2$ and 3 suggest a maximum of $\sim$20% of the total luminosity density will be lost by non-selection of $0\,\text{Å} < W_{\mathrm{Ly}\alpha} < 20$ Å galaxies, and such a selection bias can certainly not explain the magnitude of the trend observed here.

It may also be argued that lower metallicities or a flattening of the IMF may explain the trend. However, between solar and 1/50 solar metallicity the increase of $W_{\mathrm{Ly}\alpha}$ for constant SFR, a measure of the relative Lyα/UV output, is less than 50% (Raiter et al. 2010), insufficient to explain the observed increase of $f_{\mathrm{esc}}^{\mathrm{Ly}\alpha}$. To explain an increase by a factor of $\sim$4 would require a decrease of the average metallicity from solar down to less than 10^{-3} solar (Raiter et al. 2010), which seems highly unlikely.

One would also assume that a relatively higher fraction of genuine primeval galaxies would be discovered as redshift increases, and a substantial ($\sim$three-fold) enhancement of Lyα/UV may arise from preferential selection of extremely young systems (e.g., Charlot & Fall 1993; Schaerer 2003). To get this kind of enhancement a galaxy must either be observed at an age below $\sim$10 Myr or, should an episode of star formation occur superimposed on an aged stellar population, sufficient time must have elapsed for that population to fade in the UV. For this UV fading to occur, punctuated bursts of star formation would need to be separated by around the UV equilibrium timescale of $\sim$100 Myr. At $z = 6$, the universe has an age of 1 Gyr and even if all star formation were to occur in individual bursts, the chance of catching an individual galaxy at this time would be around 10%. Thus, integrated over the entire galaxy population the application of such a sampling bias also seems quite implausible.

We may expect at some point over this cosmic evolution that galaxies start to leak a substantial fraction of their ionizing photons ($f_{\mathrm{esc}}^{\mathrm{LyC}}$). Indeed, as we approach the middle of the epoch of reionization, the reionization processes itself dictates that this must be true, and we may expect at lower redshifts (e.g., 4–6) that a substantial population of galaxies may remain with an ISM that permits high $f_{\mathrm{esc}}^{\mathrm{LyC}}$. In addition, approximately across the same redshift domain we may expect the thickening neutral phase of the IGM to start to suppress Lyα. Both of these effects would act to lower the perceived Lyα escape fraction by either draining ionizing photons or scattering Lyα. Although we are not able to tell whether these effects become significant at $z \sim 4$–6; if they do become important then the intrinsic Lyα escape fractions of these galaxies will be still higher than we measure.[8]

It may be argued that the measured Lyα fluxes (and hence the Lyα luminosity density) could be underestimated due to the spatial extension of Lyα, and that some of the observed redshift trend could be due to this (e.g., Loeb & Rybicki 1999; Zheng et al. 2010). Although a somewhat larger spatial extension of Lyα compared to the UV continuum has been noted in some surveys (e.g., Nilsson et al. 2009; Finkelstein et al. 2010); stacking analysis in other *Hubble Space Telescope* images reveals the Lyα emission to be spatially compact, with only a small fraction of the integrated luminosity lost to aperture effects (Bond et al. 2010). Therefore, it seems very unlikely that this could lead to a significant underestimate of the Lyα flux, which would mimic the apparent trend of increasing Lyα escape fraction with redshift. The main reasons are the following. First, the photometric apertures typically used for the narrowband images taken from the ground are several times larger than the FWHM of the Lyα emission and several studies apply the same method at several redshifts (e.g., between $z \sim 3$ and 6, Ouchi et al. 2008). Second, several independent measurements using both imaging and spectroscopy reveal the same trend between $z \sim 2$ and 6 (Ouchi et al. 2008; Cassata et al. 2011; Stark et al. 2010a), and also over a smaller redshift range (Reddy et al. 2008). Third, it is well known that in individual Lyα-selected systems at redshifts 2–3, the SFR inferred by comparing Lyα and UV radiation is frequently found to be comparable (Guaita et al. 2010; Nilsson et al. 2009; Ouchi et al. 2008). Finally, some of the brightest Lyα-emitting objects on the sky—where the order of magnitude fainter low surface brightness scattered emission should become apparent—also seem to be spatially compact (e.g., Westra et al. 2006). These observational lines of evidence all argue against an important loss of Lyα photons related to its spatial extension.

At $z \sim 0.2$–0.4, the Lyα-emitting samples have been carefully constructed from surveys using *Galaxy Evolution Explorer* (*GALEX*) slitless spectroscopy of NUV continuum-selected objects (Deharveng et al. 2008; Cowie et al. 2010). Given its relatively low spatial resolution ($\sim$5″), the Lyα flux measurement of individual sources should not be affected by possible differences in the spatial extension. Furthermore, blending affects only 10% of the sources, according to Cowie et al. (2010). Finally, comparing number counts of *GALEX* sources with/without Lyα emission, these authors have also shown that the Lyα emitters represent only $\sim$5% of the NUV-selected continuum sources, a fraction significantly lower than the 20%–25% derived for $z \sim 3$ LBGs by Shapley et al. (2003). In other words, a low escape fraction at low-z is not only obtained from the ratio of the UV and Lyα luminosity density, but also from direct inspection of NUV continuum-selected objects.

Finally, as discussed in Section 2.2, our assumed limits of integration may introduce an overall bias into the data. For

[8] For example, assuming that half of the Lyα flux is lost due to scattering in the IGM the "intrinsic" value of $f_{\mathrm{esc}}^{\mathrm{Ly}\alpha}$ out of galaxies would be higher by a factor of 1.22 (1.92) at $z \sim 3$ (6), assuming the average IGM opacity of Madau (1995).

both the Lyα- and UV-selected populations, the characteristic luminosity of the LF ($L_\star$) is known to evolve with redshift. Thus selecting a constant lower limit at all redshifts may result in an artificial evolution. First, it should again be noted that our fixed lower limits apply to both the numerator and denominator (Lyα and UV LFs; in Equation (1)) and to first order will cancel. Second, the evolution of both Lyα and UV LFs follows a similar pattern, starting low in the nearby universe and increasing rapidly to $z = 2$ or 3, from where they begin to decline in the direction of the highest redshifts (with the Lyα LF declining slower than that of the UV in this range). Thus were this effect to be significant, and also not to cancel as just suggested, we would expect a strong upward evolution from $z \approx 0$ to 2 which we do see, followed by a slow decline to higher redshift, which is certainly not reflected in the data.

In short, the various methods and arguments all point clearly toward a significant evolution of the Lyα space fraction with redshift. The main uncertainty affecting the precise absolute value of $f_{\rm esc}^{\rm Ly\alpha}$ is probably due to statistical uncertainties in the LFs and to the simple extinction correction applied to derive it, not possible Lyα losses due to apertures.

5.2. The Downwardly Evolving Escape Fraction and the Properties of the Intergalactic Medium

Beyond a redshift of around 5.7, the measured value of $f_{\rm esc}^{\rm Ly\alpha}$ begins to decline, although initially this decline is weak and the deviation from our best-fit relationship at redshift 6.5 is not significant. Adding the $z = 6.5$ point of Ouchi et al. (2010) and Kashikawa et al. (2006) to our fit does not change the result. However, the $z = 7$ point lies at just 8%, and is around 2σ below both the best-fit $f_{\rm esc}^{\rm Ly\alpha}$–$z$ relationship (Figure 1) and the predictions at this redshift based upon the $f_{\rm esc}^{\rm Ly\alpha}$–$E_{B-V}$ relationship (Figure 3). The $z = 7.7$ point formally takes the value of $f_{\rm esc}^{\rm Ly\alpha} = 0$, and is presented with an extremely conservative error that is likely to be grossly overestimated (see Section 2.3). In comparison to $z = 5.7$, $f_{\rm esc}^{\rm Ly\alpha}$ has declined by a factor of at least two by $z = 7$. We have so far attributed the increase in $f_{\rm esc}^{\rm Ly\alpha}$ to an evolution in the dust content of galaxies, and it would be an extravagant departure from this evolutionary trend were ISM evolution to suddenly cause a sharp drop in $f_{\rm esc}^{\rm Ly\alpha}$ at $z > 6$. Several other mechanisms are, however, naturally able to explain this break in the trend.

5.2.1. Leaking Ionizing Radiation

As discussed previously and by, for example, Bunker et al. (2010) and Bouwens et al. (2010b), the LyC escape fraction at $z \sim 8$ must have been around 20%–50% in order to reionize the universe, depending upon the clumping factor of neutral hydrogen. Thus, as the galaxy population embedded in the reionization epoch evolves into the population observed at lower redshifts ($\approx$3), it must also transition through a phase of modest average $f_{\rm esc}^{\rm LyC}$ ($\approx$0.1–0.2). At these redshifts, measurements of $f_{\rm esc}^{\rm LyC}$ are emerging that do seem to be consistent with these values (Iwata et al. 2009; Vanzella et al. 2010), which continue to evolve to lower values with decreasing redshift (see Siana et al. 2010). Furthermore, since at $z \approx 7$ we are looking through the nearest edge of the reionization epoch into a partially neutral universe (as determined by quasar absorption studies, Fan et al. 2006), substantial LyC leakage must occur from the $z \sim 7$ galaxies in order to complete reionization.

If we set $f_{\rm esc}^{\rm LyC} \approx 0$ at $z = 5.7$ and hold all the other properties of the galaxy population constant (i.e., no strong evolution of galaxy metallicity or IMF), this estimate of $f_{\rm esc}^{\rm LyC} \sim 30\%$ at $z \approx 7$ would also reduce the nebular emission line spectrum to 70% of its value at $z \approx 6$. This in itself would be sufficient to bring the predicted value for $f_{\rm esc}^{\rm Ly\alpha}$ within 1σ of the measured value at $z = 7$. Thus, even in the redshifts 7–8 domain we suggest that the drop in the Lyα LF could be attributed to the drainage of ionizing photons.

5.2.2. Neutralizing the Intergalactic Medium

As the IGM shifts from ionized to neutral, Lyα photons scatter in gas that immediately surrounds galaxies (Miralda-Escude 1998; Haiman & Spaans 1999). This is expected to manifest as a drop in the observed Lyα number counts or LF (Rhoads & Malhotra 2001; Hu et al. 2002), providing a test of cosmic reionization that tails much farther back in redshift than absorption tests in quasar spectra. Previously Malhotra & Rhoads (2006) and Kashikawa et al. (2006) have used the evolution of the Lyα LF to look for such signatures of a neutral IGM transition but found conflicting results. However, the raw differential comparison of LFs only tests the ionized fraction if the evolution of the underlying galaxy population is understood to an equal, or preferably better, level and Dijkstra et al. (2007) showed that the evolution reported by Kashikawa et al. (2006) can, for example, be explained purely by the evolution of the dark matter halo population. In a similar vein to our own analysis, Stark et al. (2010b) have suggested the fraction of LBGs showing strong Lyα emission to be a preferable signature of cosmic reionization to the evolution of the Lyα LF. Furthermore, from the lack of Lyα line emission in six out of seven $z \sim 7$ galaxy candidates, Fontana et al. (2010) suggest that an increasingly neutral IGM is responsible for reversing the observed trend of the increasing fraction of strong emitters at redshift below $\sim$6.

By recasting the problem in terms of the Lyα escape fraction, we remove the question of halo evolution from the problem—any halo mass function evolution is accounted for by the LBG population that is used to compute $f_{\rm esc}^{\rm Ly\alpha}$. The drop in the Ly$\alpha$ LF is also reflected by the $f_{\rm esc}^{\rm Ly\alpha}$–$z$ diagram, quite securely by $z = 7$. If we hold the ISM properties and $f_{\rm esc}^{\rm LyC}$ constant, we see that between redshifts 6 and 8 we need to suppress $\gtrsim$50% of the Lyα luminosity. However, what this means for the neutral gas fraction is much harder to infer since the fraction of photons that scatter in the IGM depends on the exact wavelength with which Lyα is emitted (Haiman 2002; Santos 2004; Malhotra & Rhoads 2004; Verhamme et al. 2008; Dijkstra & Wyithe 2010). All we can say with reliability is that the average effective optical depth seen by emitted Lyα photons at $z \sim 7$ would be about one.

In summary, the dip in the observed Lyα escape fraction beyond a redshift of 6 seems to be real and, holding all other galaxy properties constant, a loss of around 50% of Lyα photons needs to be accounted for by $z = 7$–8. Current data can be equally well described by the galaxy population emitting this fraction of LyC photons, and by Lyα photons seeing an IGM optical depth (at the velocity of the emitting galaxy) of around 1. Observational discrimination between the two scenarios will remain extremely challenging, but basically calls for further deep spectroscopic observations of the $z = 7$–8 narrowband and dropout candidates, most likely requiring extremely large telescopes.

5.3. Evolution of the Dust Content of Galaxies

So far, we have been taking advantage of the fact that we have measurements of the dust extinction in our samples of Hα- and UV-selected galaxies. We have used this to infer the intrinsic SFRD of the populations, and from there calculated $f_{\rm esc}^{\rm Ly\alpha}$ using Equations (2) and (3). These equations connect the quantity of $f_{\rm esc}^{\rm Ly\alpha}$ with E_{B-V}, via the ratio of the Lyα- and UV-derived measurements of the SFRD, $\dot{\rho}_\star$. However, in Section 4 we defined an alternative relationship between $f_{\rm esc}^{\rm Ly\alpha}$ and E_{B-V}, based upon analyzing individual galaxies, where we provide an empirical relationship between these two quantities (Equation (4)) and relate them simply through coefficients. Thus, we have four quantities ($\dot{\rho}_\star^{\rm Ly\alpha}$, $\dot{\rho}_\star^{\rm UV}$, E_{B-V}, and $f_{\rm esc}^{\rm Ly\alpha}$) that are related by the various coefficients discussed in the previous sections.

In all the previous sections, we have made use of the measured values of E_{B-V}, but instead we could ignore this measurement and invert the problem: use the observed Lyα and uncorrected UV SFRDs at a given redshift to estimate E_{B-V}, using Equation (4) as a closure relation. Thus, substituting Equation (4) into Equation (2), we can write

$$E_{B-V} = \frac{1}{0.4(k_\lambda - k_{\rm Ly\alpha})} \times \log_{10}\left(\frac{\dot{\rho}_{\star,{\rm Ly\alpha}}^{\rm Obs}}{\dot{\rho}_{\star,{\rm UV}}^{\rm Obs} \times C_{\rm Ly\alpha}}\right). \quad (6)$$

Out to $z \approx 6$ we take the data compiled in Table 1, and compute the observed SFRD from either Hα or the UV, depending on the redshift. We then use Equation (6) to estimate the sample-averaged E_{B-V} at each redshift, independently of the attenuation measurements themselves. In short, we ignore the fact that these E_{B-V} measurements have been made, and see if we can recreate them. We show the result as black data points in the upper panel of Figure 4, with the actual measurements shown by the small gray symbols. We then hypothesize that the dust content of the universe may decrease exponentially, and adopting a function of the form $E_{B-V}(z) = C_{\rm EBV} \cdot \exp(z/z_{\rm EBV})$, we fit the coefficients $C_{\rm EBV} = 0.386$ and $z_{\rm EBV} = 3.42$. Or, the e-folding redshift scale for the E_{B-V} evolution is $\approx$3.4. We show this relationship in Figure 4 with the thick red line.

By performing this experiment we are throwing away observational information and the plot becomes somewhat noisier, but nevertheless it resembles an inverted version of Figure 1. Fundamentally, the plot shows a decrease in the E_{B-V} of galaxies as redshift increases, which is consistent with the measurements (Table 1 and gray points). This decrease in the dust content of galaxies with redshift is already much discussed in the literature for LBGs at $z \sim$ 2–7 based upon a gradual blueing of the UV slopes (e.g., Hathi et al. 2008; Bouwens et al. 2009). At higher redshift, there is however a tendency for our new method to estimate higher E_{B-V} compared to the measurements obtained directly from the UV stellar continuum. In the upper panel of Figure 4, we also show the best-fitting relationships derived in the previous sections (black solid line), where we take the redshift evolution of $f_{\rm esc}^{\rm Ly\alpha}$ and use Equation (4) to convert to E_{B-V} using our best-fit coefficients—naturally, this line almost perfectly reproduces the gray points.

The red line (fit to these data) runs slightly flatter than the black one (combined fits from the previous sections) and suggests a slightly higher E_{B-V}, and therefore dust content, than measured at the highest redshifts in Bouwens et al. (2009). At $z \sim$ 3–6 however, it runs lower than the measurements of

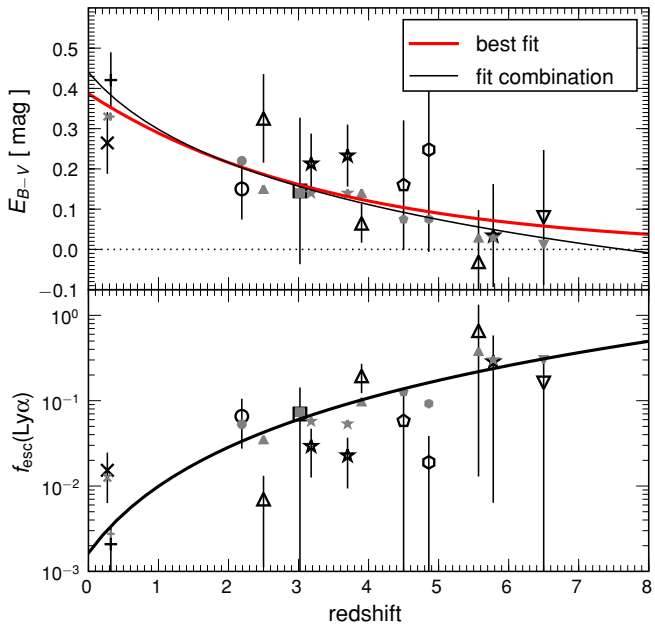

Figure 4. Upper: the evolution of the dust content of galaxies with redshift. Black points show E_{B-V} derived from the raw observed (i.e., not dust corrected) SFRDs in Lyα and the UV (also Hα) using Equation (6). The gray points show the actual measured values which in general are well reproduced by our new method. The black line shows the predictions based upon the $f_{\rm esc}^{\rm Ly\alpha}$–$z$ and $f_{\rm esc}^{\rm Ly\alpha}$–$E_{B-V}$ relationships derived in Sections 3 and 4, respectively. The red line shows the best-fitting exponential function to these (black) data points, and is shown to run slightly flatter, predicting more dust at higher redshifts. Lower: E_{B-V} measurements from the upper plot, but translated into $f_{\rm esc}^{\rm Ly\alpha}$ using our $f_{\rm esc}^{\rm Ly\alpha}$–$E_{B-V}$ relationship (Equation (4) and Figure 2). The gray points show the same data as Figure 1; the black line shows the preferred $f_{\rm esc}^{\rm Ly\alpha}$–$z$ power law. The figure demonstrates that we would have arrived at approximately the same conclusions, even if we had no measurements other than the Lyα and UV LFs. (A color version of this figure is available in the online journal.)

Hathi et al. (2008), who obtain slightly higher dust attenuations from LBG samples.

It is interesting to further investigate how the dust obscurations we derive compare with other estimates. The SPH modeling of Nagamine et al. (2010) and Dayal et al. (2009) already discussed in Section 3.2 both predict higher dust attenuations than measured in the $z = 6$ dropout populations at $E_{B-V} =$ 0.15. Detailed SED modeling of $z \sim$ 6–8 galaxies by Schaerer & de Barros (2010) also suggest the presence of dust in some high-z LBGs. Here, we estimate $E_{B-V} \approx 0.08$ based upon the new methodology. Similarly the semi-analytical approach developed in Baugh et al. (2005) find $E_{B-V} \sim 0.1$ at $z > 3$ when examining the LBG population, which is certainly compatible with our estimates in the redshifts 3–5 domain.

Since the empirical relationship derived between $f_{\rm esc}^{\rm Ly\alpha}$ and E_{B-V} relates the two quantities directly, for completeness we convert our E_{B-V} redshift estimates to $f_{\rm esc}^{\rm Ly\alpha}$ through Equation (4). This enables us to approximately re-create the main observational result of this article, Figure 1, which we show in the lower panel of Figure 4. Here, we show the $f_{\rm esc}^{\rm Ly\alpha}$ estimates derived in this section with black shapes, with the original points from Figure 1 shown in gray. In short the difference between the two sets of points is that in the gray ones, the measured dust attenuation has been applied to the UV SFRD in the computation of $f_{\rm esc}^{\rm Ly\alpha}$ whereas in the black points, this quantity has been estimated directly from the observed SFRDs, using Equation (6). As with Figure 1 this shows $f_{\rm esc}^{\rm Ly\alpha}$ increasing

with redshift, but the actual estimates of the dust attenuation in the individual samples have not been used in the derivation of this figure. The overall trend of Figure 1 is maintained, although significant scatter has been added to the plot. It shows that even were no E_{B-V} measurements available, our main result would have taken the same form and the overall trend would have been the same.

6. SUMMARY

We have compiled fifteen Lyα LFs from the literature between redshifts 0 and 8 and integrated them over homogeneous limits to obtain Lyα luminosity densities. We have performed the same calculations with Hα-emitting galaxies at $z \lesssim 2.3$, and with UV-selected/dropout samples at $z > 2.3$, together with their extinctions due to dust. We subsequently used these dust-corrected luminosity densities to estimate the sample-averaged volumetric Lyα escape fraction ($f_{\rm esc}^{\rm Ly\alpha}$) as a function of redshift. In summary, we show:

1. That $f_{\rm esc}^{\rm Ly\alpha}$ increases monotonically from the $\lesssim$1% level at $z \approx 0$ to around 40% by redshift 6. Over this redshift range, the evolution can be well described by a power law of the form $f_{\rm esc}^{\rm Ly\alpha}(z) = C \times (1+z)^{\xi}$, for which we obtain coefficients of $C = (1.67^{+0.53}_{-0.24}) \times 10^{-3}$; $\xi = (2.57^{+0.19}_{-0.12})$. This relationship predicts that $f_{\rm esc}^{\rm Ly\alpha}$ should reach unity by a redshift of $z = 11.1^{+0.8}_{-0.6}$.
2. By combining samples of galaxies at redshifts 2–3 for which $f_{\rm esc}^{\rm Ly\alpha}$ and E_{B-V} have been computed, we derive a new empirical relationship between these quantities. This provides an effective attenuation law for Lyα photons that includes not only the effects of dust absorption, but also those of resonance scattering by neutral hydrogen. This new relationship takes the form $f_{\rm esc}^{\rm Ly\alpha} = C_{\rm Ly\alpha} \times 10^{-0.4 \cdot E_{B-V} \cdot k_{\rm Ly\alpha}}$, where $k_{\rm Ly\alpha} = 13.8$ and $C_{\rm Ly\alpha} = 0.445$.
3. By combining our new $f_{\rm esc}^{\rm Ly\alpha}$–$E_{B-V}$ relationship with the measured dust content of (UV- and Hα-selected) samples in our study, we predict how $f_{\rm esc}^{\rm Ly\alpha}$ should evolve with redshift, making no reference to Lyα observations. Between redshifts 0 and 6.5, we find that this prediction is fully consistent with our measurements. Thus we are able to relate the upward redshift evolution of $f_{\rm esc}^{\rm Ly\alpha}$ to the general decrease in the dust content of the galaxy population. We discuss other effects that could mimic this trend, but ultimately find all of them to be implausible.
4. Beyond a redshift of 6 we see a drop in $f_{\rm esc}^{\rm Ly\alpha}$ that amounts to a factor of 2–4 by redshift 8. As has been done previously, we discuss this drop in terms of an increasing neutral gas fraction of the IGM, but now stress that by casting the problem as one of $f_{\rm esc}^{\rm Ly\alpha}$, we mitigate the question of halo mass evolution from diagnostic tests of cosmic reionization. We note however, that the drop in $f_{\rm esc}^{\rm Ly\alpha}$ could also be explained by a volumetric escape of ionizing photons of $f_{\rm esc}^{\rm LyC} \approx 50\%$, which has also been implied at $z = 7.5$ by recent observations. Unfortunately, an observational diagnostic test between the two scenarios will remain extremely challenging.
5. Using the observed trend between $f_{\rm esc}^{\rm Ly\alpha}$ and E_{B-V} derived at $z = 2$, we find a relationship between the observed ratio of Lyα/UV SFRDs and the quantity E_{B-V}. We then use the raw measurements of $\dot{\rho}_\star$ (Lyα and uncorrected UV) to estimate how the dust content of galaxies evolves with redshift. Our result is a general decrease in dust with increasing redshift, but not as fast a decrease as measured in UV-selected samples. This decline is well fit by an exponential function of the form $E_{B-V}(z) = C_{\rm EBV} \exp(z/z_{\rm EBV})$, where $C_{\rm EBV} = 0.386$ and $z_{\rm EBV} = 3.42$. Using this method, the dust contents we derive at $z = 3$–6 are consistent with those found by semi-analytical and SPH models of galaxy formation.

M.H. and D.S. are supported by the Swiss National Science Foundation. G.Ö. is a Swedish Royal Academy of Sciences research fellow supported by the Knut and Alice Wallenberg foundation, and also acknowledges support from the Swedish research council (VR). J.M.M.-H. is funded by Spanish MICINN grants CSD2006-00070 (CONSOLIDER GTC) and AYA2007-67965. D.K. and H.A. are supported by the Centre National d'Etudes Spatiales (CNES). We thank Mark Dijkstra and Mauro Giavalisco for useful feedback on the manuscript.

REFERENCES

Adams, T. F. 1972, ApJ, 174, 439
Ahn, S., Lee, H., & Lee, H. M. 2003, MNRAS, 340, 863
Ajiki, M., Mobasher, B., Taniguchi, Y., Shioya, Y., Nagao, T., Murayama, T., & Sasaki, S. S. 2006, ApJ, 638, 596
Ajiki, M., et al. 2004, PASJ, 56, 597
Arnouts, S., et al. 2005, ApJ, 619, L43
Atek, H., Kunth, D., Hayes, M., Östlin, G., & Mas-Hesse, J. M. 2008, A&A, 488, 491
Atek, H., Kunth, D., Schaerer, D., Hayes, M., Deharveng, J. M., Östlin, G., & Mas-Hesse, J. M. 2009, A&A, 506, L1
Baugh, C. M., Lacey, C. G., Frenk, C. S., Granato, G. L., Silva, L., Bressan, A., Benson, A. J., & Cole, S. 2005, MNRAS, 356, 1191
Blanc, G. A., et al. 2010, arXiv:1011.0430
Bond, N. A., Feldmeier, J. J., Matković, A., Gronwall, C., Ciardullo, R., & Gawiser, E. 2010, ApJ, 716, L200
Bouwens, R. J., Illingworth, G. D., Franx, M., & Ford, H. 2007, ApJ, 670, 928
Bouwens, R. J., et al. 2009, ApJ, 705, 936
Bouwens, R. J., et al. 2010a, ApJ, 708, L69
Bouwens, R. J., et al. 2010b, ApJ, 709, L133
Brocklehurst, M. 1971, MNRAS, 153, 471
Bunker, A. J. 2010, MNRAS, 409, 855
Calzetti, D., Armus, L., Bohlin, R. C., Kinney, A. L., Koornneef, J., & Storchi-Bergmann, T. 2000, ApJ, 533, 682
Cassata, P., et al. 2011, A&A, 525, 143
Charlot, S., & Fall, S. M. 1993, ApJ, 415, 580
Cowie, L. L., Barger, A. J., & Hu, E. M. 2010, ApJ, 711, 928
Dawson, S., Rhoads, J. E., Malhotra, S., Stern, D., Wang, J. X., Dey, A., Spinrad, H., & Jannuzi, B. T. 2007, ApJ, 671, 1227
Dayal, P., Ferrara, A., & Saro, A. 2010, MNRAS, 402, 1449
Dayal, P., Ferrara, A., Saro, A., Salvaterra, R., Borgani, S., & Tornatore, L. 2009, MNRAS, 400, 2000
Deharveng, J., et al. 2008, ApJ, 680, 1072
Dijkstra, M., & Wyithe, J. S. B. 2010, MNRAS, 408, 352
Dijkstra, M., Wyithe, J. S. B., & Haiman, Z. 2007, MNRAS, 379, 253
Dunkley, J., et al. 2009, ApJS, 180, 306
Fan, X., Carilli, C. L., & Keating, B. 2006, ARA&A, 44, 415
Finkelstein, S. L., Rhoads, J. E., Malhotra, S., & Grogin, N. 2009, ApJ, 691, 465
Finkelstein, S. L., Rhoads, J. E., Malhotra, S., Grogin, N., & Wang, J. 2008, ApJ, 678, 655
Finkelstein, S. L., et al. 2010, arXiv:1008.0634
Fontana, A., et al. 2010, ApJ, 725, L205
Giavalisco, M., Koratkar, A., & Calzetti, D. 1996, ApJ, 466, 831
Gronwall, C., et al. 2007, ApJ, 667, 79
Guaita, L., et al. 2010, ApJ, 714, 255
Haiman, Z. 2002, ApJ, 576, L1
Haiman, Z., & Spaans, M. 1999, ApJ, 518, 138
Hansen, M., & Oh, S. P. 2006, MNRAS, 367, 979
Harrington, J. P. 1973, MNRAS, 162, 43
Hartmann, L. W., Huchra, J. P., & Geller, M. J. 1984, ApJ, 287, 487

Hathi, N. P., Malhotra, S., & Rhoads, J. E. 2008, ApJ, 673, 686
Hayes, M., et al. 2010a, Nature, 464, 562
Hayes, M., Schaerer, D., & Östlin, G. 2010b, A&A, 509, L5
Hibon, P., et al. 2010, A&A, 515, A97
Hu, E. M., Cowie, L. L., Capak, P., McMahon, R. G., Hayashino, T., & Komiyama, Y. 2004, AJ, 127, 563
Hu, E. M., Cowie, L. L., McMahon, R. G., Capak, P., Iwamuro, F., Kneib, J.-P., Maihara, T., & Motohara, K. 2002, ApJ, 568, L75
Isobe, T., Feigelson, E. D., & Nelson, P. I. 1986, ApJ, 306, 490
Iwata, I., et al. 2009, ApJ, 692, 1287
Iye, M., et al. 2006, Nature, 443, 186
Kashikawa, N., et al. 2006, ApJ, 648, 7
Kennicutt, R. C., Jr. 1992, ApJ, 388, 310
Kennicutt, R. C., Jr. 1998, ARA&A, 36, 189
Kornei, K. A., Shapley, A. E., Erb, D. K., Steidel, C. C., Reddy, N. A., Pettini, M., & Bogosavljević, M. 2010, ApJ, 711, 693
Kunth, D., Lequeux, J., Sargent, W. L. W., & Viallefond, F. 1994, A&A, 282, 709
Kunth, D., Mas-Hesse, J. M., Terlevich, E., Terlevich, R., Lequeux, J., & Fall, S. M. 1998, A&A, 334, 11
Laursen, P., Sommer-Larsen, J., & Andersen, A. C. 2009, ApJ, 704, 1640
Le Delliou, M., Lacey, C. G., Baugh, C. M., & Morris, S. L. 2006, MNRAS, 365, 712
Le Delliou, M., et al. 2005, MNRAS, 357, L11
Leitherer, C., et al. 1999, ApJS, 123, 3
Loeb, A., & Rybicki, G. B. 1999, ApJ, 524, 527
Madau, P. 1995, ApJ, 441, 18
Malhotra, S., & Rhoads, J. E. 2004, ApJ, 617, L5
Malhotra, S., & Rhoads, J. E. 2006, ApJ, 647, L95
Mas-Hesse, J. M., Kunth, D., Tenorio-Tagle, G., Leitherer, C., Terlevich, R. J., & Terlevich, E. 2003, ApJ, 598, 858
Meurer, G. R., Heckman, T. M., & Calzetti, D. 1999, ApJ, 521, 64
Miralda-Escude, J. 1998, ApJ, 501, 15
Nagamine, K., Ouchi, M., Springel, V., & Hernquist, L. 2010, PASJ, 62, 1455
Neufeld, D. A. 1990, ApJ, 350, 216
Neufeld, D. A. 1991, ApJ, 370, L85
Nilsson, K. K., Tapken, C., Møller, P., Freudling, W., Fynbo, J. P. U., Meisenheimer, K., Laursen, P., & Östlin, G. 2009, A&A, 498, 13
Ono, Y., et al. 2010, ApJ, 724, 1524
Orsi, A., Lacey, C. G., Baugh, C. M., & Infante, L. 2008, MNRAS, 391, 1589
Osterbrock, D. E. 1962, ApJ, 135, 195
Östlin, G., Hayes, M., Kunth, D., Mas-Hesse, J. M., Leitherer, C., Petrosian, A., & Atek, H. 2009, AJ, 138, 923
Ota, K., et al. 2008, ApJ, 677, 12
Ouchi, M., et al. 2004, ApJ, 611, 660
Ouchi, M., et al. 2008, ApJS, 176, 301
Ouchi, M., et al. 2010, ApJ, 723, 869
Raiter, A., Schaerer, D., & Fosbury, R. 2010, A&A, 523, 64
Reddy, N. A., Steidel, C. C., Pettini, M., Adelberger, K. L., Shapley, A. E., Erb, D. K., & Dickinson, M. 2008, ApJS, 175, 48
Rhoads, J. E., & Malhotra, S. 2001, ApJ, 563, L5
Santos, M. R. 2004, MNRAS, 349, 1137
Santos, M. R., Ellis, R. S., Kneib, J., Richard, J., & Kuijken, K. 2004, ApJ, 606, 683
Scarlata, C., et al. 2009, ApJ, 704, L98
Schaerer, D. 2003, A&A, 397, 527
Schaerer, D., & de Barros, S. 2010, A&A, 515, A73
Schechter, P. 1976, ApJ, 203, 297
Schiminovich, D., et al. 2005, ApJ, 619, L47
Shapley, A. E., Steidel, C. C., Pettini, M., & Adelberger, K. L. 2003, ApJ, 588, 65
Shimasaku, K., et al. 2006, PASJ, 58, 313
Shioya, Y., et al. 2009, ApJ, 696, 546
Siana, B., et al. 2010, ApJ, 723, 241
Stark, D. P., Ellis, R. S., Chiu, K., Ouchi, M., & Bunker, A. 2010a, MNRAS, 408, 1628
Stark, D. P., Ellis, R. S., & Ouchi, M. 2010b, arXiv:1009.5471
Tapken, C., Appenzeller, I., Noll, S., Richling, S., Heidt, J., Meinköhn, E., & Mehlert, D. 2007, A&A, 467, 63
Tapken, C., et al. 2006, A&A, 455, 145
Tasitsiomi, A. 2006, ApJ, 645, 792
Thuan, T. X., & Izotov, Y. I. 1997, ApJ, 489, 623
Tilvi, V., Malhotra, S., Rhoads, J. E., Scannapieco E., Thacker R. J., Iliev, I. T., & Mellema, G. 2009, ApJ, 704, 724
Tresse, L., & Maddox, S. J. 1998, ApJ, 495, 691
van Breukelen, C., Jarvis, M. J., & Venemans, B. P. 2005, MNRAS, 359, 895
Vanzella, E., et al. 2010, ApJ, 725, 1011
Venemans, B. P., Kurk, J. D., & Miley, G. K., et al. 2002, ApJ, 569, L11
Verhamme, A., Schaerer, D., Atek, H., & Tapken, C. 2008, A&A, 491, 89
Verhamme, A., Schaerer, D., & Maselli, A. 2006, A&A, 460, 397
Wang, J. X., Malhotra, S., & Rhoads, J. E. 2005, ApJ, 622, L77
Westra, E., et al. 2006, A&A, 455, 61
Zheng, Z., Cen, R., Weinberg, D., Trac, H., & Miralda-Escude, J. 2010, arXiv:1010.3017